Agricultural and Forest Meteorology 168 (2013) 186–200

Contents lists available at SciVerse ScienceDirect

Agricultural and Forest Meteorology

journal homepage: www.elsevier.com/locate/agrformet

Long-distance dispersal of spruce budworm (*Choristoneura fumiferana* Clemens) in Minnesota (USA) and Ontario (Canada) via the atmospheric pathway

Brian R. Sturtevant[a,*], Gary L. Achtemeier[b], Joseph J. Charney[c], Dean P. Anderson[d], Barry J. Cooke[e], Philip A. Townsend[f]

[a] USDA Forest Service, Northern Research Station, Institute for Applied Ecosystem Studies, 5985 Hwy K, Rhinelander, WI 54501, USA
[b] USDA Forest Service, Southern Research Station, Forestry Sciences Laboratory, Athens, GA 30602-2044, USA
[c] USDA Forest Service, Northern Research Station, East Lansing, MI 48823, USA
[d] Landcare Research, P.O. Box 40, Lincoln, New Zealand
[e] Canadian Forest Service, 5320-122nd Street, Edmonton, AB T6H 3S5, Canada
[f] Department of Forest and Wildlife Ecology, University of Wisconsin–Madison, Madison, WI 53706, USA

ARTICLE INFO

Article history:
Received 28 July 2011
Received in revised form 16 August 2012
Accepted 7 September 2012

Keywords:
Spruce budworm
Choristoneura fumiferana
Long-distance dispersal
Aerobiology
Agent-based modeling

ABSTRACT

Dispersal can play an important role in the population dynamics of forest insects, but the role of long-distance immigration and emigration remains unclear due to the difficulty of quantifying dispersal distance and direction. We designed an agent-based spruce budworm flight behavior model that, when interfaced with temperature, wind speed, and precipitation output from a high-resolution atmospheric model, produces detailed flight trajectories and deposition patterns over large landscapes. Rules and relationships describing budworm adult (moth) lift-off, ascent, horizontal flight, and descent were parameterized using a detailed empirical study of budworm dispersal behavior and corresponding meteorological conditions during a 1970s outbreak in New Brunswick, Canada. Simulated moth landings were assumed to be dependent in part on the availability of suitable host tree species. We applied the model to a 6.4 million ha landscape at the border between northern Minnesota (USA) and Ontario (Canada) during an eight-day flight window in late June 2007. Specimens collected during and after this flight window indicated moths emerging from an inland source of outbreak populations dispersed over 150 km to trap sites near the north shore of Lake Superior, where localized cooling was predicted to have delayed emergence of locally-produced budworm moths. Simulations suggested immigration of moths to lakeshore sites from the outbreak source was plausible on three of eight dates within the flight window, but the relatively narrow deposition footprints implied immigration occurred on different dates across lakeshore sites. Apart from wind speed and direction, precipitation and low temperatures limited dispersal to substantially shorter distances for a few dates within the simulated flight window. Key uncertainties limiting our understanding of atmospheric transport of spruce budworm include behavioral responses to vertical heterogeneity in the air temperature profile, the precipitation threshold required for the forced descent of moths from the air column, and search mechanisms affecting host and/or mate location during long-distance flight.

Published by Elsevier B.V.

1. Introduction

The ability to disperse long-distances is fundamental to the population ecology of most economically-important insect pests (Isard and Gage, 2001). Yet the role of long-distance dispersal in the spread, synchrony, and persistence of insect outbreaks remains unclear due to the difficulty of quantifying dispersal and its impacts on populations (Royama, 1979, 1984; Royama et al., 2005). For Lepidopteran forest defoliators, dispersal has been indirectly inferred by examining egg to moth ratio, which can indicate exodus by dispersers from heavily defoliated areas (Nealis and Régnière, 2004; Royama, 1984; Royama et al., 2005). Theoretical models testing dispersal parameters have produced spatial covariance estimates of populations matching observed defoliation patterns (e.g., Williams and Liebhold, 2000). In these models, dispersal was usually represented as a stationary process (i.e. parameters are equal over the entire landscape); however, mounting evidence suggests that dispersal is not stationary (Keyghobadi et al., 1999, 2006). Spatial factors affecting insect movement may include landscape structure (Cooke and Roland, 2000; Nathan et al., 2005), vegetation phenology (Gage et al., 1999), temperature (Sanders et al., 1978), and the direction and speed of air currents (Anderson and Sturtevant,

* Corresponding author. Tel.: +1 715 362 1105; fax: +1 715 362 1166.
E-mail address: bsturtevant@fs.fed.us (B.R. Sturtevant).

0168-1923/$ – see front matter. Published by Elsevier B.V.
http://dx.doi.org/10.1016/j.agrformet.2012.09.008

2011; Greenbank et al., 1980; Onstad et al., 2003). However, the actual influence of dispersal on spatiotemporal patterns of insect outbreaks is a hotly contested area of research (e.g., Royama et al., 2005) and will remain so until dispersal processes can be quantified more precisely.

Most forest and agricultural pests either actively or passively use wind to enhance their dispersal (e.g., Greenbank et al., 1980; Onstad et al., 2003; Riley et al., 1991; Westbrook and Isard, 1999). Aerobiology – the science of the atmospheric transport of biota – requires understanding of ecology, life history, behavior, meteorology, and the multiple scales at which these factors interact (Gage et al., 1999). To date aerobiology has been most often applied to understand the passive transport of biota, particularly pollen (Bohrerova et al., 2009; Schueler and Schlunzen, 2006) and pathogen spores (Isard et al., 2005, 2007; Waggoner and Aylor, 2000). Actively dispersing insects, including many economically important pest species (Strand, 2000), add complexity by introducing behaviors during ascent, horizontal transport, and descent stages of the atmospheric dispersal pathway. Empirical observations of flight behaviors from field studies (Greenbank et al., 1980), radar (e.g., Chapman et al., 2010; Greenbank et al., 1980; Riley et al., 1991; Westbrook and Isard, 1999), and laboratory experiments (Lu et al., 2007; Vogt et al., 2000; Wu et al., 2006) may be used to empirically estimate key flight behaviors such as time of ascent, flight duration, velocity parameters, thermal and energetic constraints for a variety of flying insects. Such studies may be used to parameterize flight models that can interface with high-resolution weather models to produce accurate patterns of insect deposition and identify source populations of immigrants (Achtemeier, 1996; Scott and Achtemeier, 1987). Coupled atmospheric-behavior models have been applied to understand avian flight behavior (Mandel et al., 2008, 2011; Sapir et al., 2011; Shamoun-Baranes et al., 2010), but only rarely applied to examine active insect dispersal through the atmospheric pathway (e.g., gypsy moth, Fossberg and Peterson, 1986; Isard and Gage, 2001).

The spruce budworm (SBW) is a native Lepidopteran that periodically defoliates balsam fir (*Abies balsamea*) and spruce species (*Picea* spp.) in the boreal and sub-boreal forests of North America. Pupation occurs between mid-June and late July, where the specific phenology is dependent on ambient temperature (Régnière and You, 1991). Adults emerge approximately 10 days after pupation with female emergence lagging a few days behind males. Adult dispersal occurs in the evenings and is dependent upon meteorological conditions (Greenbank et al., 1980; Régnière and Nealis, 2007), and levels of host defoliation (Nealis and Régnière, 2004; Royama, 1984). Both sexes emigrate together with similar exodus characteristics, though the sex ratio of emigrants is biased toward females (Greenbank et al., 1980). Adult females select either spruce or fir for oviposition, but do not indicate preference between spruce and fir species (Régnière and Nealis, 2007). Adults are strong fliers and can easily disperse 20 km with a maximum recorded dispersal distance of 450 km (Greenbank et al., 1980).

In this paper we describe the design and application of an atmospheric transport model for SBW adult (moths). SBW is one of the few species for which aerobiological parameters have been empirically estimated in situ under outbreak population conditions (Greenbank et al., 1980). We applied the SBW transport model to an eight-day flight window in northern Minnesota and adjacent Ontario corresponding with budworm adult male capture data from a large spatial network of pheromone traps. We evaluated model behavior by addressing the question: What is the prospect that budworm adults emerging from a localized outbreak in northern Minnesota dispersed to moth collection sites over 150 km to the east on the lakeshore of Lake Superior, where SBW phenology is generally delayed due to lake-effect cooling? This question was evaluated by the relative proximity of simulated moth landings relative to six lakeshore trapping sites, and by quantifying the flight properties (i.e., distance, direction, relative landing success etc.) of simulated moths over the flight period.

2. Methods

2.1. Model description

2.1.1. Lagrangian trajectory model

The SBW atmospheric transport model is an agent-based model of budworm flight, where each agent is representative of an insect or group of insects with the same flight characteristics, assigned behavioral parameters based on probability distribution functions corresponding to the timing of liftoff, relative flight strength, and descent rules (see Section 2.1.2). The Lagrangian trajectory model calculates a step-by-step location of the SBW agent flight through a four-dimensional wind field simulated by a numerical meteorological model. The trajectory model is diagnostic in that trajectories are calculated from meteorological model output as opposed to embedding the agent within the meteorological model during its production run. Meteorological model outputs used to construct the trajectories consist of a time series of simulated temperature, wind speed, wind direction, and precipitation concentration for regularly spaced point locations on a horizontal grid and vertically spaced sigma levels subject to compression in the surface layer with the compression being relaxed with height. In our specific application we applied the Weather Research and Forecasting Model (WRF v3, Skamarock et al., 2005) to produce outputs for a 6.5 million ha study area at hourly intervals at grid points spaced at 4 km in the horizontal and 50 vertically stretched sigma levels below 3000 m above ground level (AGL), with 33 of the levels packed within the lowest 1000 m AGL (see Section 2.2.1). The input map consists of a bitmap image file, referred to thereafter as the "study map", with three cell types corresponding with source habitat, host target habitat, and the remaining matrix.

Each segment of the agent trajectory from launch to landing (or transport out of the grid domain) is calculated through a "predictor-corrector" method for streamlines (Achtemeier, 1979) adapted for trajectories (Scott and Achtemeier, 1987). The construction of a trajectory segment of an agent located at $P(x_0,y_0,z_0,t_0)$ through a time and space-varying wind field to a new spatial and temporal location $P(x,y,z,t)$ ($t = t_0 + \Delta t$) proceeds along the following steps. The current position $P(x_0,y_0,z_0,t_0)$ is enclosed by two square cuboids each defined by eight corner points of the meteorological grid and enclosing the hour interval of the weather model output that bounds t_0. Thus 16 points are involved in the construction of the trajectory segment. While passage of the trajectory segment through the side of the cuboid or past the weather time step complicates the mathematical bookkeeping, the methodology is the same. Each of the 16 corner points carries the components of the vector wind for its three-dimensional location and weather output interval. The values for wind vector components at x_0,y_0,z_0,t_0 are calculated by linear interpolation of the components at the 16 corner points to construct the vector wind V_0 at $P(x_0,y_0,z_0,t_0)$. The flight velocity components of the SBW adult agent, dependent on the flight stage of the insect (see Section 2.1.2), are then added to the wind vector components to construct the flight-modified wind vector V_0' components at $P(x_0,y_0,z_0,t_0)$ using the following equations:

$$u_0' = \begin{cases} (V_0 + H_i) \times \sin\left(\frac{\pi}{180} \times \alpha_0\right) & \text{ascent and horizontal flight statges} \\ V_0 \times \sin\left(\frac{\pi}{180} \times \alpha_0\right) & \text{descent stages} \end{cases} \quad (1)$$

$$v_0' = \begin{cases} (V_0 + H_i) \times \cos\left(\frac{\pi}{180} \times \alpha_0\right) & \text{ascent and horizontal flight stages} \\ V_0 \times \cos\left(\frac{\pi}{180} \times \alpha_0\right) & \text{descent stages} \end{cases} \quad (2)$$

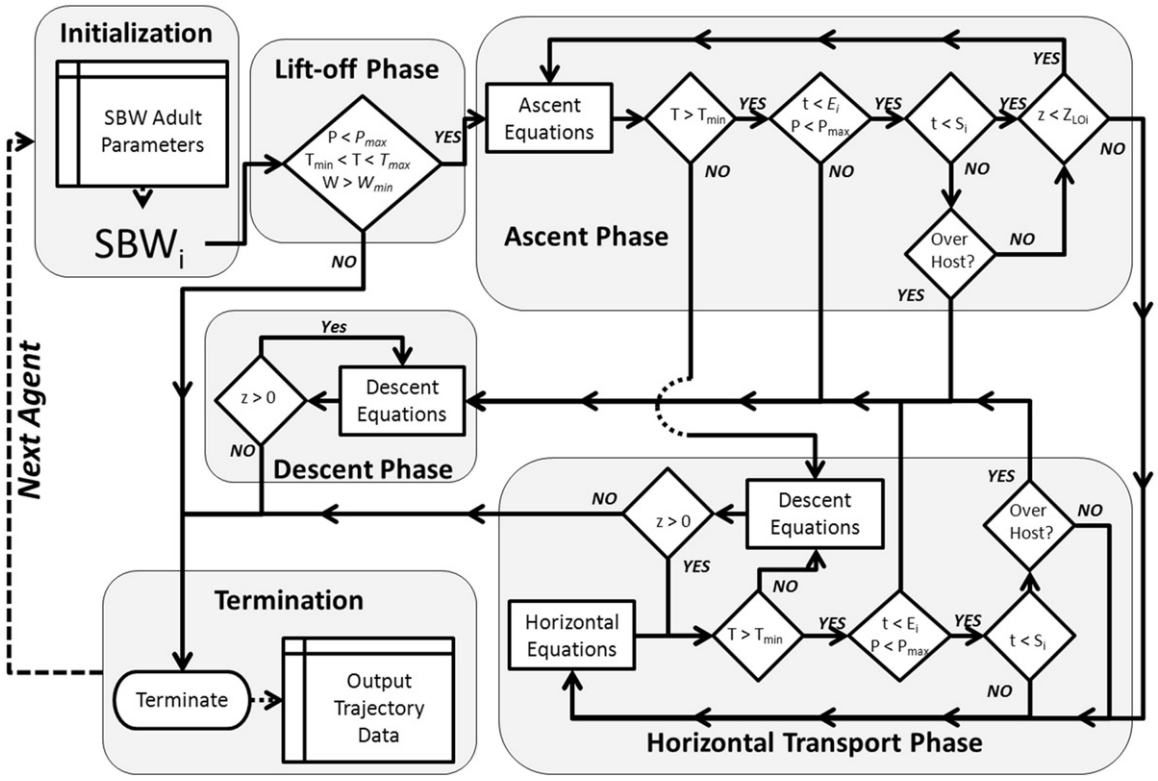

Fig. 1. Model flow diagram illustrating the logic of the spruce budworm flight behavior model. See Table 1 for parameter descriptions and values. Ascent, horizontal, and descent equations are delineated in Eqs. (1–3).

$$w_0' = \begin{cases} V_0 + A_i & \text{ascent stages} \\ V_0 & \text{horizontal flight stages} \\ V_0 - D_i & \text{descent stages} \end{cases} \quad (3)$$

where α_0 is the downwind direction in degrees, u_0', v_0', and w_0' are the flight-modified east-west, north-south, and vertical components of V_0' at $P(x_0,y_0,z_0,t_0)$, and H_i, A_i, and D_i are the horizontal flight, ascent, and descent velocities for the ith SBW adult (see Table 1 for parameter descriptions and values). The components of V_0' are then used to estimate a new location, $P(x_1, y_1, z_1, t) = P(x_0, y_0, z_0, t_0) + V_0' \cdot \Delta t$, where Δt is the time step of the trajectory algorithm, set at 10 s. A new vector wind V_1 is estimated at the new location via linear interpolation of the wind vector components among the sixteen corner points to time t, and the flight velocity components at time t are added to construct the flight-modified wind vector V_1' at $P(x_1,y_1,z_1,t)$ using Eqs. (1–3) and substituting in the components of V_1. The components of the initial insect-modified wind vector (V_0') are then averaged with the components of the estimated insect-modified wind vector (V_1') to get V components (i.e., the predictor-corrected vector components u, v, and w). The components of V are then used to calculate the trajectory segment end point from $P(x_0,y_0,z_0,t_0)$ to $P(x,y,z,t)$, adding a small random factor to the components of V to approximate neglected subscale meteorological processes and variations in agent flight:

$$P(x) = P(x_0) + \{u[1 + U(-0.1, 0.1)]\} \times \Delta t \quad (4)$$

$$P(y) = P(y_0) + \{v[1 + U(-0.1, 0.1)]\} \times \Delta t \quad (5)$$

$$P(w) = P(z_0) + \{w[1 + U(-0.1, 0.1)]\} \times \Delta t \quad (6)$$

where U is a random uniform number with interval from −0.1 to 0.1. The process then repeats for the next trajectory segment starting at its new location.

The model first generates a table of SBW adult agents with stochastic parameters randomly assigned within the ranges indicated in Table 1, where the number of agents simulated is defined by the number of source cells and the number of agents potentially launched per source cell. The model constructs flight trajectories sequentially for each record in the initialized table, and outputs the resulting trajectory attributes including lift-off success or failure, cause and coordinates of failed lift-offs, source and termination coordinates for each successful lift-off, cause of descent, lift-off and landing time, maximum altitude, coordinates for location of maximum altitude, and whether the SBW adult successfully landed within host habitat (Fig. 1).

2.1.2. Flight behavior rules and parameters

Rules and parameters comprising the SBW flight behavior model govern the four active phases of SBW migration: liftoff, ascent, transport, and descent (Isard et al., 2005) (Fig. 1). Parameters controlling these rules come primarily from Greenbank et al. (1980), who coordinated ground and air-based collections of dispersing SBW with meteorological measurements and radar studies to demonstrate the importance of air temperature, wind speed, and wind direction on SBW adult dispersal in New Brunswick, Canada (Table 1).

The liftoff time for the ith agent, L_i, on a given day is randomly selected from a truncated Gaussian distribution L:

$$L \sim Normal(t_p, \sigma^2) \qquad t_b \le L \le t_e \quad (7)$$

where t_b and t_e correspond with beginning and end times, respectively, defining the flight window (Greenbank et al., 1980), and function L is defined by the mean (i.e., peak) lift-off time t_p and variance σ^2 in decimal hours. Peak lift-off is temperature-dependent (i.e., earlier on cool nights) and is estimated as a linear function of

Table 1
Parameter values for the SBW atmospheric transport model with descriptions and literature sources.

Parameter (units)	Symbol	Value	Description and source[a]
Earliest lift-off (decimal h)	t_b	18.5	Earliest observed lift-off time; p. 17
Peak lift-off (decimal h)	t_p	Calculated	Peak lift-off time estimated as a function of temperature at t_b; p. 17
Lift-off variance (decimal h^2)	σ^2	6.1	Daily variation in lift-off time. Estimated from same source as t_p
Latest lift-off (decimal h)	t_e	23.5	Latest observed lift-off time; p. 17
Minimum temperature (°C)	T_{min}	15	Minimum air temperature for lift-off and active flight; p. 15, Sanders et al. (1978)
Maximum temperature (°C)	T_{max}	29.5	Maximum air temperature for lift-off; p. 15
Minimum wind speed (m s^{-1})	W_{min}	0.7	Minimum wind speed for lift-off (20 m above ground); p. 15
Maximum precipitation (mm h^{-1})	P_{max}	2.5	Moths do not lift-off during "heavy rain"; p. 15; Moths deposited prematurely by heavy precipitation; p. 21
Ascent velocity (m s^{-1})	$A_0(\pm\Delta A)$	0.6(±0.1)	Vertical ascent velocity (p. 18) with strong vs. weak flier variation
Level-off height (m)	z		Distribution derived
Mode		200	from Schaefer (1976)
Range		0–500	
Horizontal velocity (m s^{-1})	$H(\pm\Delta H)$	2(±0.5)	Moth flight velocity in the downwind direction (p. 20) with strong vs. weak flier variation
Searching time (h)	S		Time after which flying moths begin hunting for host trees.
Early hunt window		0.5–1	Three temporal windows define the time at which individuals begin hunting for host. Upon finding host hunting moths initiate descent; p. 21
Mid-hunt window		1–3	
Late hunt window		3–6	
Maximum flight duration	E	6(±0.5)	Average longest duration (p. 20) with variation defining exhaustion rule
Descent velocity (m s^{-1})	D	2.0	Moth descent velocity described as "well in excess of 1 m s^{-1}"; p. 21)

[a] Page numbers refer to Greenbank et al. (1980).

the temperature at 19.5 h LST (T_b) and t_p (Greenbank et al., 1980, p. 17),

$$t_p = 12.67 + 0.33T_b \quad (8)$$

Agent lift-off is then subject to three constraints assessed at the time (L_i) and location for each agent: surface temperatures are within the temperature range for active moth flight ($T_{min} \le T \le T_{max}$) (Sanders et al., 1978; Greenbank et al., 1980); wind speed at 20 m above ground level is above the minimum value (W_{min}) defining "calm winds"; and precipitation at the ground level is below the precipitation threshold (P_{max}) defining "heavy rain" (Table 1). All constraints must be met for lift-off to occur (Fig. 1).

The ascent phase initiates at lift-off and ends when the moth reaches its level-off height or is forced to descend (Fig. 1). Level-off height (z_{LOi}) is selected from a probability function (Z_{LO}) that replicates the vertical distribution of airborne moths documented under stable air mass conditions (Schaefer, 1976) (Fig. 2). We assumed that ascent velocity for the ith moth, A_i, varies uniformly with the mean velocity A measured by Greenbank et al. (1980) and interval defined as $\pm\Delta A$ to account for differences between weak and strong fliers within the SBW population (Achtemeier, 2002; Table 1)

The horizontal flight phase is defined as the period of time from level-off until initiation of descent behavior that culminates with the insect returning to the ground (Fig. 1). As with ascent velocity, horizontal flight velocity ith moth, H_i, is selected from a uniform distribution with mean H defined by Greenbank et al. (1980) and interval defined as $\pm\Delta V$ (Table 1). Horizontal flight is assumed to be in the downwind direction during both ascent and horizontal phases based (Eqs. 1–3), where the minor variations in moth orientation from the downwind angle (Greenbank et al., 1980) are assumed to be integrated into the random factor applied in Eqs. (4–6). The descent phase is defined as the period of time from the initiation of descent behavior that culminates in the insect returning to the ground to the termination of the flight trajectory at ground level. Ground observers and radar from the Greenbank et al. (1980) study documented nearly vertical descent of moths, suggesting that SBW moths may sense their hosts (i.e., spruce and fir) below and drop out of the air column into suitable oviposition sites. We assumed that at some time during transport the moths actively begin searching for host, where the assigned "searching time" for a given agent was randomly selected from one of three time periods (0.5–1.0 h, 1.0–3.0 h, and 3.0–6.0 h; Table 1) (Greenbank et al., 1980). When an agent in searching mode detects host trees along its migratory pathway, it folds its wings and descends to the ground at its descent velocity (D; Table 1; Greenbank et al., 1980).

Three factors may trigger premature descent behavior in either ascent or horizontal transport phases: minimum temperature, precipitation, and exhaustion constraints (Fig. 1). We assumed the

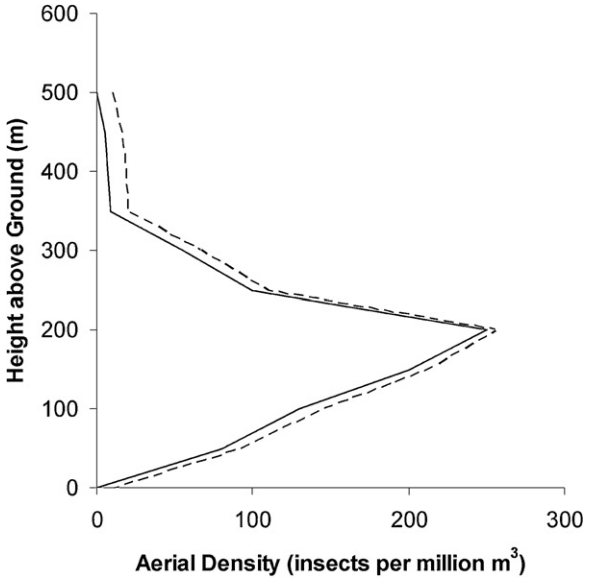

Fig. 2. The vertical distribution of SBW reported at 2117 LST 6 July 1973 in New Brunswick representative of SBW flight altitude under stable air masses (Schaefer, 1976) (solid line), and the simulated distribution of maximum altitude (Z_{max}) based on 10,000 iterations of the SBW transport model (dashed line) offset by 10 insects.

same minimum temperature limiting lift-off also limits active flight (Sanders et al., 1978) (T_{min}; Table 1). Below this threshold temperature the insect will descend until it either reaches air temperatures above T_{min} and can maintain level flight or reaches the ground surface (Fig. 1). Heavy rainfall has also been observed to cause premature deposition of SBW (Dickison et al., 1983, 1986). The rate of precipitation necessary to "wash" moths from the air column is not known, and while numerical weather prediction models do predict the formation and movement of precipitation echoes, the spatial and temporal accuracy of model-generated precipitation echoes is problematic. We therefore applied a conservative estimate of 2.5 mm h^{-1} as the minimum amount of rain that could conceivably cause premature deposition also constrain lift-off (Table 1). Empirical and anecdotal evidence suggests that flying moths will eventually reach a maximum flight duration beyond which they will descend due to exhaustion (Greenbank et al., 1980). Using their observations, we estimated the exhaustion time for agent i (E_i) as 6 h plus a random number between 0 h and 0.5 h, giving each insect a maximum flight window that ranges from L_i to $L_i + E_i$. With the exception of the minimum temperature constraint, active descent behavior is assumed to continue once initiated until the insect reaches the ground surface (Fig. 1).

2.2. Model evaluation

We evaluated the model results by comparing simulated moth flight properties and landing patterns with a spatiotemporal pattern of actual moth trap captures within a large landscape with vastly different local phenologies and population densities. Such differences provided opportunity to infer the identity of immigrants and their source of emigration. A temporal series of SBW moth collections from 2007 was available for a 6.5 million ha forested region straddling the USA–Canadian border between Minnesota and Ontario (Anderson and Sturtevant, 2011) (Fig. 3). The study area is dominated by a continental climate with long, cold winters and relatively short summers, and a physiography characterized by abundant lakes and gentle relief (Heinselman, 1973). However, Lake Superior has a strong moderating effect on the climate of its lake shore, resulting in cooler spring and summer temperatures relative to areas further inland. Such lakeshore cooling will delay budworm phenology (Régnière and You, 1991). In 2007, the closest outbreak population of SBW to the lakeshore of Lake Superior was over 100 km inland to the west (Fig. 3). Hence early moth captures from phenologically delayed areas around Lake Superior are most likely explained by rapid atmospheric transport of moths from a specific geographic source.

2.2.1. Insect sampling and phenology

SBW adult males were collected at 120 sites distributed across the study area (Anderson and Sturtevant, 2011). Three traps baited with polyethylene caps containing eastern SBW pheromone (E-11-Tetradecenal; Z-11-Tetradecenal; Scentry Biologicals, Inc.) and containing insecticidal vaportape (Dimethyl-2,2-dichlorovinyl phosphate; Hercon Environmental) were placed at each sample site. A combination of universal traps (UniTrap) and Multipher 1 traps (approximately equal numbers of each) that have similar moth capture rates (Mullen et al., 1998) were used. Traps were hung at approximately 1.5 m above ground surface from branches of balsam fir or white spruce approximately 5–10 m apart in mid-June 2007. Moths were removed from traps in road-accessible areas every 7–10 days during the main flight period (late June through mid-July) and at a final collection at the end of August. Within the large central wilderness areas without road access (Fig. 3), samples were collected once during a two-week period from early to mid-August. We applied SBW phenology model (BioSIM 9.5, Régnière and Amant-Saint, 2004; Régnière and You, 1991) to the study area using a network of 222 unique real-time weather stations (Environment Canada, 2009; National Oceanic and Atmospheric Administration, 2009) and a 30 m resolution digital elevation model (Canadian Council on Geomatics, 2009; U.S. Geologic Survey, 2009) to map predicted moth emergence dates and expected daily trap captures for the study area.

Table 2
WRF parameterizations used in this study.

Process	WRF parameterizations
Microphysics	Lin et al. scheme (Lin et al., 1983)
Cumulus	Kain–Fritsch (Kain and Fritsch, 1993)
Planetary boundary layer	Mellor Yamada Janjić (MYJ) (Janjic, 1996, 2002; Mellor and Yamada, 1982)
Surface layer	MYJ (Janjic, 1996, 2002; Mellor and Yamada, 1982)
Land surface	Noah (Chen and Dudhia, 2001)
Radiation	Rapid Radiative Transfer Model for longwave radiation (Mlawer, 1997) Dudhia for shortwave radiation (Dudhia, 1989)

2.2.2. Weather modeling

We simulated weather conditions representing the time of the first moth collection (21 June–29 June 2007), using the Weather Research and Forecasting Model (WRF v3, Skamarock et al., 2005), to provide the weather inputs required to drive the SBW atmospheric transport model, following parameterizations listed in Table 2. Model inputs included gridded analyses of meteorological conditions from the time period of interest as initial and boundary conditions, as well as topography, vegetation type, and other land surface characteristics. Outputs for this study consisted of hourly three-dimensional grids of simulated wind speed, wind direction, air temperature, and precipitation. We employed the NCEP North American Regional Reanalysis (Mesinger et al., 2006) to supply initial and boundary conditions for a 36 km grid spacing outer domain, which covered most of the United States, southern Canada, and northern Mexico (Fig. 3). Two one-way nested grids at 12 km and 4 km grid spacing (Fig. 3) provided increasing spatial resolution over the region of interest. All of the results presented in this paper derive from the 4 km grid run at a 10 s time step. This configuration of the WRF employs 50 vertically stretched sigma levels, with 33 of the levels packed within the lowest 1000 m AGL (3-6 m vertical grid spacing at the ground surface to approximately 250 m vertical grid spacing at 1000 m AGL) to provide additional detail in atmospheric layers that are most important for simulating the dispersal of SBW moths.

We produced a series of four 48-h WRF simulations starting at 0000 Universal Time, Coordinated (UTC) [1900 the previous day Local Daylight Time (LDT)], on 21, 23, 25, and 27 of June 2007. WRF simulation employed a 12-h "spin-up" to minimize the effects of imbalances in the initial conditions on the meteorological fields passed to the interface model. Hourly output from the 4 km grid was extracted for the study area and used to drive the SBW atmospheric interface model. To document differences between the WRF simulation and observed weather conditions within the study area, we compared hourly time series of simulated surface temperature, wind speed, and wind direction to corresponding observations collected at Ely, MN, and 12-h (0000 and 1200 UTC) outputs simulated at 800 m above International Falls, MN for comparison with corresponding rawinsonde balloon observations (Fig. 3). We also compared hourly surface wind speed, direction, and precipitation observations from 12 Remote Automatic Weather Stations (RAWS; http://www.raws.dri.edu/) with simulated SBW adult deposition patterns to evaluate the degree to which surface observations corresponded with simulated SBW flight behaviors as they responded

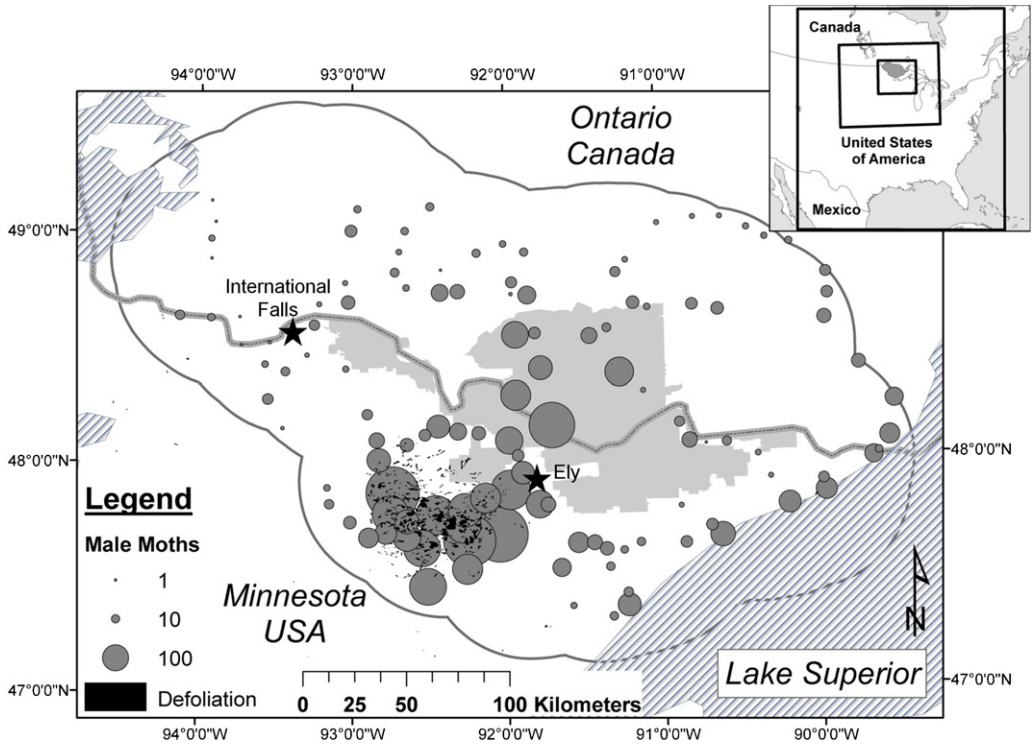

Fig. 3. Border lakes study area, showing total number of adult males captured in pheromone traps in summer of 2007. Light shading indicates wilderness areas without road access, and dark shading shows budworm defoliation documented by aerial surveys (U.S. Forest Service, 2007). The inset shows the nested spatial domains for the weather simulations (outer = 36 km, middle = 12 km, inner = 4 km grid spacing), and stars show locations for weather validation data.

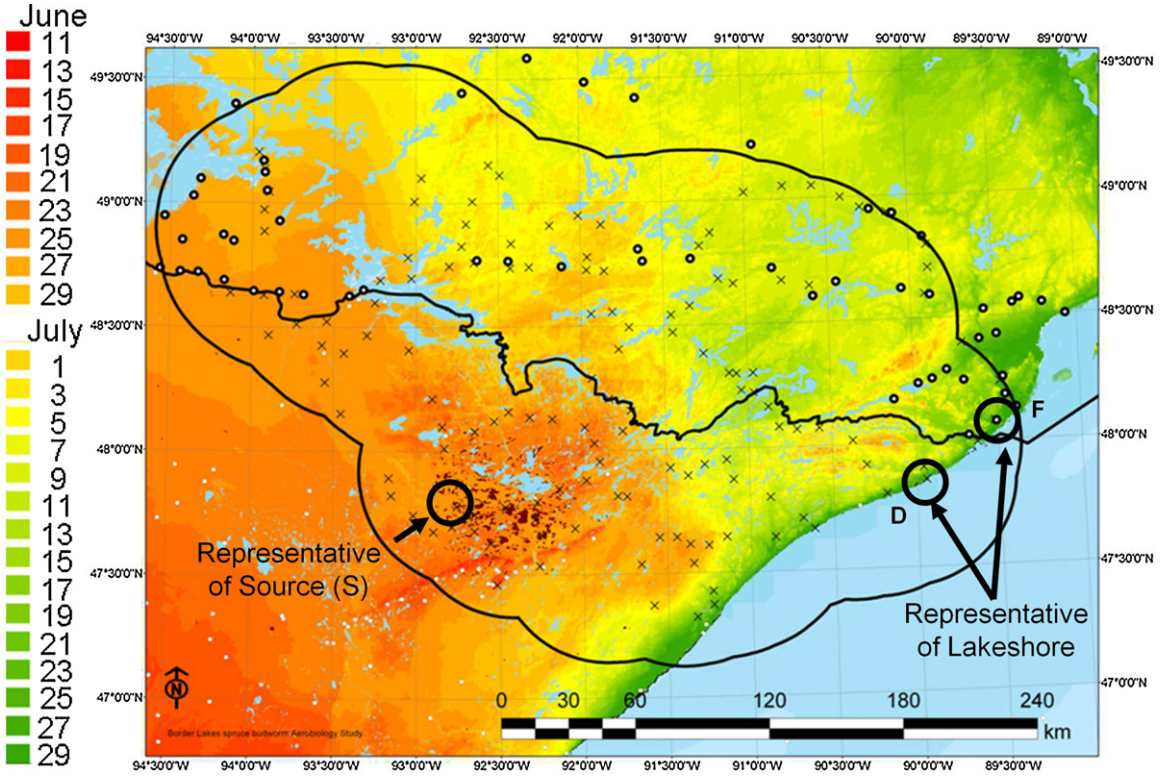

Fig. 4. BioSIM estimates for adult male spruce budworm trap catch based on weather-related phenology for source area (represented by site S) and two sites representative of lakeshore phenology (sites D and F). Meteorological stations used to estimate phenology are indicated by white dots and white dots encircled in bold for American and Canadian stations, respectively. Insect collection sites are indicated by × symbols.

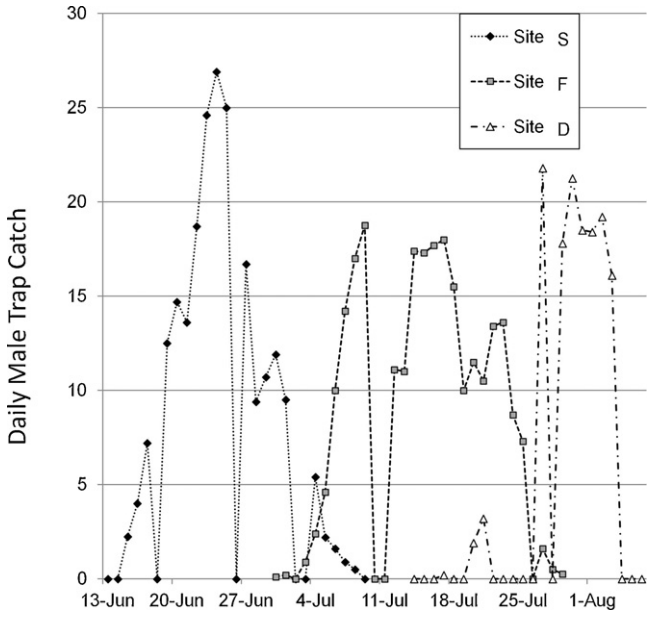

Fig. 5. Peak adult emergence dates in 2007, as estimated by BioSIM, mapped for the study area. Site S is representative of the phenology of SBW within the source area defined by detectable defoliation. Sites D and F are evaluation sites along the lakeshore where adult emergence was not anticipated until after the simulated dispersal period (ending 28 June).

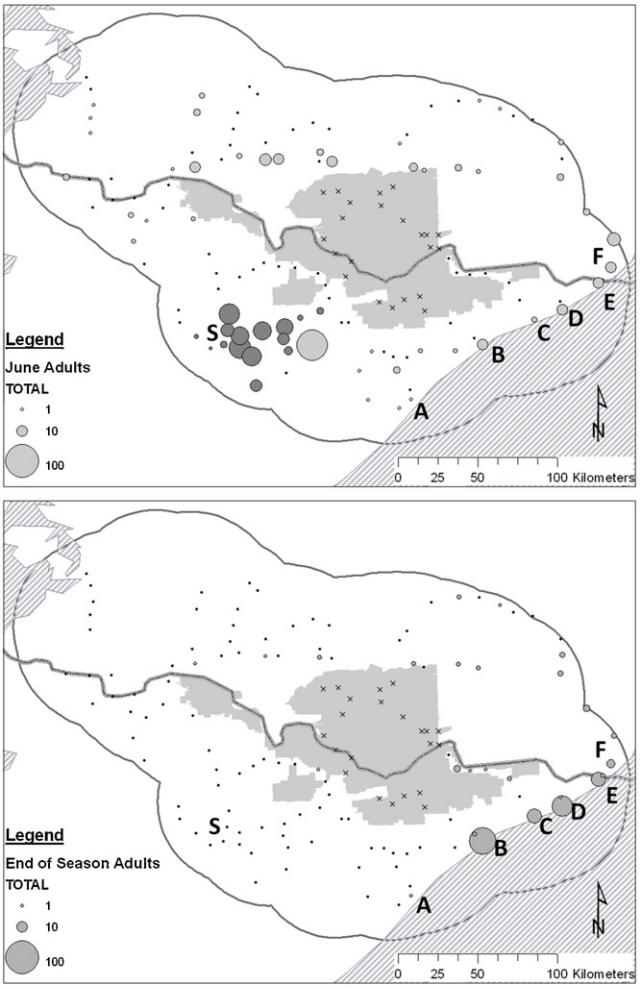

Fig. 6. (a) Number of adult males captured on 22 June (dark gray) and between 25 and 29 June (light gray) (all dates in 2007); (d) late season adult males captured after 19 July. Solid dots represent zero captures. × symbols are wilderness sites with only a single moth collection date (late July–early August). Letter labels indicate sites phenologically representative of the source (S) and the lakeshore (A–F).

to WRF outputs. All subsequent times are reported in LDT (i.e., UTC – 0500 hr).

2.2.3. Input maps and model outputs

Mass-exodus (i.e., long-distance dispersal) behavior in SBW is thought to be contingent on declining food resources (Régnière and Nealis, 2007). Mapped defoliated areas indicating tree defoliation should therefore be reasonable surrogates for sources of adult emigrants. Host target habitat may be derived from forest composition maps derived from satellite classifications or other sources, such as forest inventories. Areas mapped as defoliated in 2007 (Fig. 3, U.S. Forest Service, 2007) defined the source cells (n = 2119, resolution = 9 ha) for emigrating moths, where a single SBW adult was launched from each source cell (n = 2119). Potential immigration target cells for dispersing adult SBW were derived from maps of spruce and fir relative basal area, produced for the study area via analysis of Landsat Thematic Mapper imagery for the entire study area circa 2005 (Wolter et al., 2008). Target cells were defined as 9 ha cells where the majority of the original 0.09 ha pixels contained were dominated by spruce, fir, or a combination of the two species. SBW moth attributes were summarized for each date, including rates of lift-off failure, rates of failure to land on host, and combined success rate, defined as successfully launched moths that landed on host target cells. Flight properties including maximum trajectory altitude and Euclidean distances from source to destination were summarized using box plot diagrams and compared with the spatial deposition patterns with respect to suspected immigration sites. We assumed a simulated landing within 5 km of a trap site indicated immigration to that site was plausible on that date.

3. Results

3.1. Budworm observations

SBW phenology estimated by BioSIM suggested a gradual trend from early emergence in the southwest to later emergence in the northeast, as well as a steep gradient associated with Lake Superior, where moth emergence near the lake shore was expected over a month later than locations further inland (Fig. 4). Predictions of daily moth trap capture for three representative sites (site S from the main defoliation zone and sites D and F adjacent Lake Superior) output by BioSIM indicated little temporal overlap in predicted moth trap captures (Fig. 5). However, moths were captured at all three sites in late June (Fig. 6a), corresponding with the primary flight period of site S but prior to the flight periods for sites D and F. Specifically, the first sample date in the defoliated area occurred on 22 June 2007. First sample dates for traps outside the defoliation area started immediately to the west on 25 June 2007, and proceeded clockwise around the study area ending on 29 June 2007 along the north shore of Lake Superior. Estimated moth emergence at sites D and F was not estimated until after this first collection date (Fig. 5), and the other lakeshore sites show similar moth phenology (Fig. 4). Late season trap captures collected after 19 July 2007 were consistent with BioSIM predictions, with high trap captures very close to Lake Superior, and a few adults captured at higher elevations and latitudes (Figs. Fig. 4 and Fig. 6b). Collectively these observations suggest that June captures of SBW moths near north shore of Lake Superior originated from locations further inland with more advanced phenology. For evaluation purposes, we identified six sites (A–F, Fig. 6) within 5 km of the lakeshore as immigration sites.

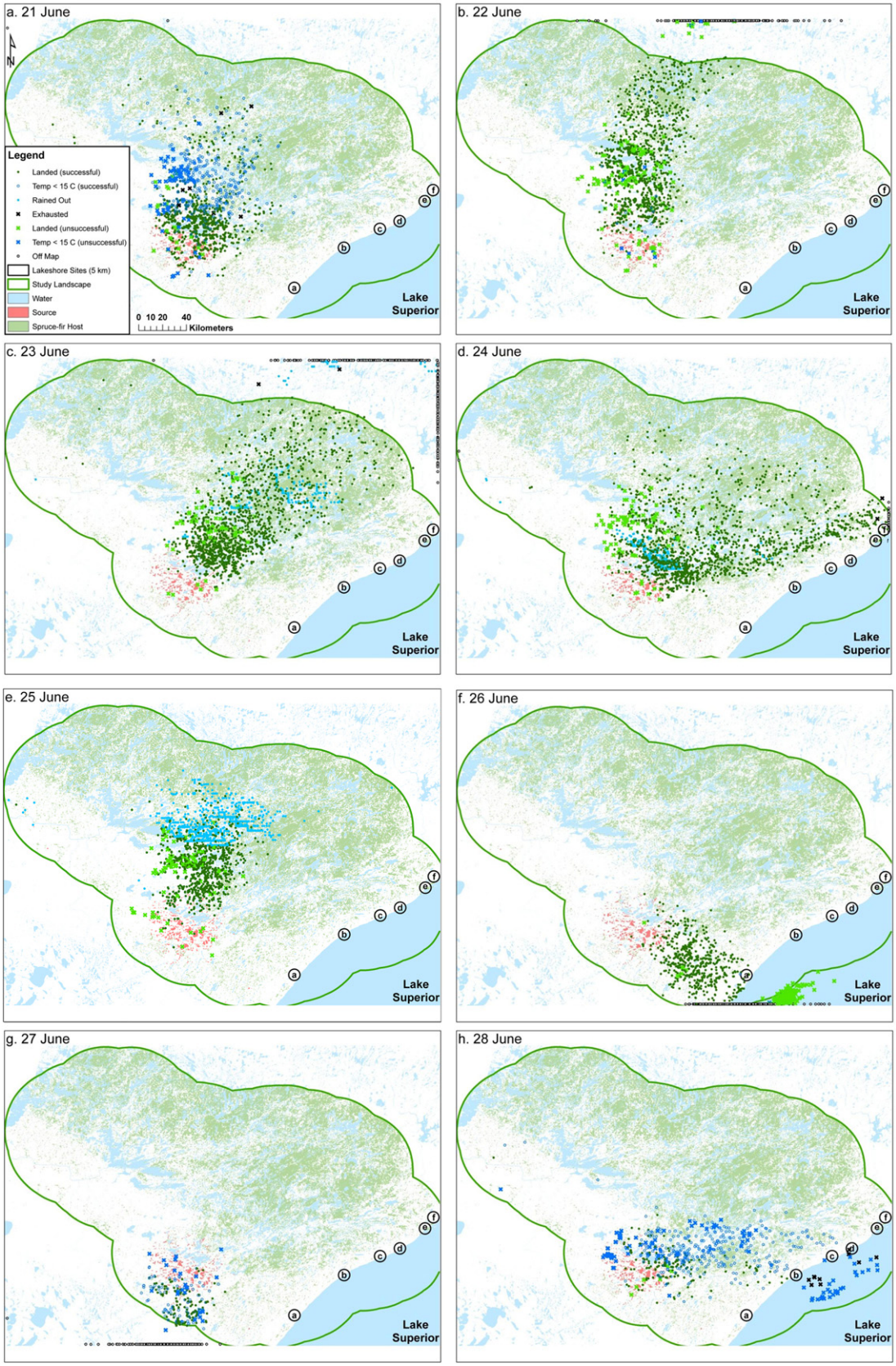

Fig. 7. Simulated moth deposition patterns by date, where different symbol and color combinations reflect the cause of landing and the success of the SBW adult in landing within spruce and fir dominated habitat. Circles indicate a 5 km radius from lakeshore evaluation sites.

3.2. Flight window meteorology

At 1900 20 June (LDT), a surface cold front passed through the upper U.S. Midwest, and northwesterly winds prevailed in the study region. Behind the front, temperatures were cooler than normal for the season and prevailed in the study area through 1900 June 24, when the winds gradually turned to a southwesterly direction. Southwesterly and southerly winds contributed to warmer and drier conditions for the following 48 h, until another cold front approached from the northwest, accompanied by stronger winds and higher relative humidities. On 25 June a cold front passed through the study area from northwest to southeast, accompanied by increasing cloudiness and rainfall. For the remainder of the dispersal window, high pressure built again while westerly and northwesterly winds contributed to cool and dry conditions.

3.3. Simulated dispersal patterns

Simulated dispersal patterns were consistent with observed synoptic weather patterns (Fig. 7). Cool temperatures limited both lift-off and dispersal distance on 21, 22, 26, and especially 27 and 28 June (Fig. 7; Table 3). 23 June dispersal patterns reflected the strong southwesterly winds on this date, resulting in a sparsely distributed deposition of moths to the northeast of the source region and over 16% of moths flying 225–325 km to the northeastern extent of the study area map (Fig. 7c). Simulations indicated SBW adult transport to the lake shore of Lake Superior was plausible on 24 June, with landings observed within 5 km of sites E and F (Fig. 7d, Table 3). Deposition patterns were strongly affected by precipitation on 25 June, where SBW adult transport was limited to less than 100 km to the north of the source (Fig. 7e). The passing cold front shifted SBW adult transport to the south and east for the remainder of the dispersal window (Fig. 7f–h). Landings were observed within 5 km of lakeshore site A on 26 June (Fig. 7f) and site D on 28 June (Fig. 7h). Sites B and C were the only sites without observed landings within 5 km (Table 3), though they clearly fall within the flight pathway on 28 June (Fig. 7h). Cool temperatures limited the number of dispersers and, combined with low wind speeds, also limited dispersal distances for that date (Table 3). SBW moths were collected from sites A–F the following day as part of our five-day collection period. Our model results indicate that lakeshore sites were within the range of dispersal distances and also consistent the direction of wind flow during the dispersal window corresponding with our collection dates. They also suggest lakeshore immigration was not due to a single event, but rather three different dispersal dates with restricted geographic extents.

Maximum altitudes on two dates (21 and 27 June) indicated vertical uplift within the wind vectors (Fig. 8). The highest maximum altitude exceeded 1000 m and all dates included at least some outlier moths with maximum altitudes in excess of 500 m (i.e., greater than the input parameters for leveling-off). Dispersal distances were positively correlated with maximum altitude across all dates (Fig. 8). Moths flying at higher altitudes also had a directional bias further clockwise in comparison with moths flying at lower altitudes (Fig. 9a). On 24 June this bias resulted in divergent flight directions, with most low-flying moths travelling north, and most high-flying moths travelling east over the higher elevations near the lake shore (Fig. 9b). Hence meteorological factors affecting uplift of moths in the air column have consequences for both the direction and magnitude of dispersal.

Despite clear differences in host abundance in different directions surrounding the source area (Fig. 7), the success rate of moths to land within host-dominated stands was only partially related to dispersal direction. Host-landing success was highest on 21 June when relatively light winds carried moths north over abundant host, and lowest on 25 June when precipitation washed three

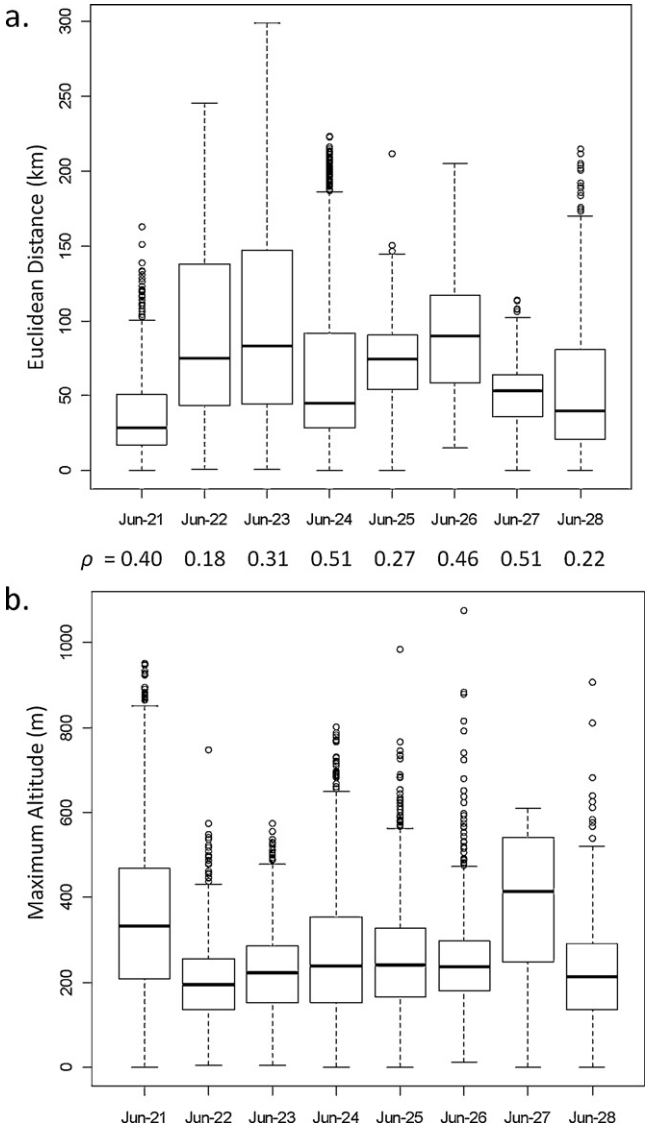

Fig. 8. Box and whisker distributions of (a) Euclidean distance traveled and (b). maximum altitude attained by SBW adults across simulation dates. Heavy lines represent median values, the box is defined by upper and lower quartiles, and the ends of the whiskers contain the range of values with extreme values identified as circles. Pearson's correlation coefficient (ρ) between variables on the different dates are indicated between the graphs.

quarters of the moths from the air (Table 3). Premature descent due to temperature also lowered host-landing success, particularly in areas with low abundance of host (Fig. 7, Table 3). Simulations from 26 June suggest that Lake Superior also acts as an important barrier affecting dispersal success. From this, it appears that the interaction between landscape patterns of host relative to the source and meteorological factors such as wind direction and flight constraints (temperature and precipitation) ultimately affect dispersal success.

3.4. Caveats

The temperature time series indicates that the WRF model was able to reproduce the diurnal cycle and daily trends in temperature at the surface, including the drop in temperature following the passage of the cold front (Fig. 10a). Daily amplitude in temperature was often overestimated at the surface relative to observed data, resulting in either warmer daytime or colder night time temperatures than expected for this area (Fig. 10a). Lift-off on the evening of 27

Table 3
Frequencies of the fates of simulated SBW moths ($n = 2119 \times 8$ nights) across dates within the dispersal window, including percent lift-off failure, missed host, and successful landings, and proximity of landings to lakeshore trap sites.

			June 2007							
			21	22	23	24	25	26	27	28
No lift-off	$T < 15\,^{\circ}C$		378	399	0	0	0	240	1117	1450
	$T > 29.5\,^{\circ}C$		0	0	23	19	7	0	0	0
	Wind $< 0.7\ m\ s^{-1}$		0	0	0	0	0	0	0	0
	Precipitation $> 2.5\ mm\ h^{-1}$		0	0	0	5	0	0	0	0
Premature descent	$T < 15\,^{\circ}C$	Host	420	14	0	0	0	1	91	352
		Nonhost	48	8	0	0	0	4	25	102
	Precipitation $> 2.5\ mm\ h^{-1}$	Host	0	0	106	33	377	0	0	0
		Nonhost	0	0	88	352	738	0	0	0
Full trajectory	Landed agent	Host	1204	1216	1473	1584	882	549	132	177
		Nonhost	21	119	53	80	82	191	0	6
	Exhausted agent		7	0	2	1	0	0	0	10
Study area limitations[a]	Beyond study landscape		0	8	42	1	0	0	6	0
	Reached study map border		2	326	327	30	0	559	463	1
Technical error[a]	Interpolation error		39	29	5	14	33	575	285	21
% Lift-off failure			17.8	18.8	1.1	1.1	0.3	11.3	52.7	68.4
% Missed host			4.5	9.4	8.3	21.1	39.4	26.2	10.1	18.2
% Total success[b]			78.5	73.6	90.7	78.0	60.4	65.5	42.5	25.8
Lakeshore landing sites[c]			–	–	–	E, F	–	A	–	D

[a] Moths failing to complete trajectories due to study area and technical limitations were removed from landing and dispersal failure/success rates.
[b] Percent of moths that successfully dispersed and landed within spruce-fir host
[c] Indicates at least one moth landed within a 5 km radius of the lakeshore trapping site identified by its letter (see Fig. 8).

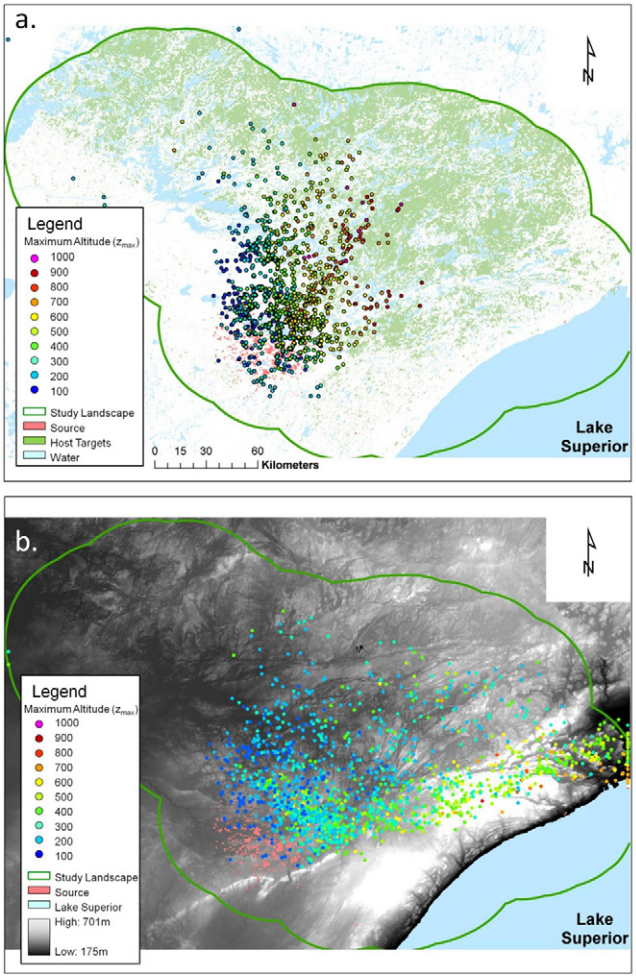

Fig. 9. (a) Moth landings for 21 June 2007 classified according to their maximum altitude during flight. (b) Moth landings for 24 June 2007 classified by maximum altitude and overlaid on topographic elevation.

June was most affected by this observed discrepancy, but this date had little bearing on our evaluation as windflow carried moths to the south outside the study area and away from the lakeshore. The 800 m AGL temperature time series at International Falls, MN also indicates the passage of the cold front, and shows general agreement between the WRF model and observation. Both observed and simulated diurnal cycles were substantially weaker at 800 m AGL than at the surface (Fig. 10d). While moth dispersal was sensitive to cold temperatures (Table 3), WRF closely matched observed temperatures with respect to the 15 °C T_{min} threshold affecting lift-off and flight at both the surface and 800 m. Simulated wind speed and wind direction also indicated strong agreement with observations at both the surface (Fig. 10b,c) and 800 m AGL with the largest exceptions occurring during daylight hours (Fig. 10d,e). WRF overestimated the wind speed when the observed wind speed was very low. This discrepancy may have affected lift-off success on 21 June and 28 June. Surface observations from RAWS stations indicated locally heavy precipitation at a few locations to the north of the source area between 2200 23 June and 0200 24 June, and then widespread precipitation during the morning daylight hours of 26 June. These observations are consistent with the premature decent caused by precipitation the night of 23 June, but suggests WRF simulated light precipitation on 24 June when none was observed, and that it simulated the precipitation event following the passage of the front approximately 12 h earlier than actually observed.

The boundary of our study area limited the maximum distance that moths could disperse. On half of the dates in the flight window a significant number (>15%) of moths flew to the rectangular extent of the study area map (Table 3). This issue was most important when winds came from the north given that the source area was close to the southern boundary of the study area. While maximum dispersal distances cannot be assessed within the limitations of this study, we can say that dispersal in excess of 300 km is possible given strong wind conditions. There was also one technical limitation, where dispersing moths located directly over a weather grid point aborted due to inability of the interface model to interpolate across points under this circumstance. Aborted flights were most numerous on the 2 dates (June 26 and 27) when wind speeds were low, accounting for terminations of as many as 27% of the launched moths (Table 3). On all other dates this technical issue affected less than 2% of the launched moths. Those moths that

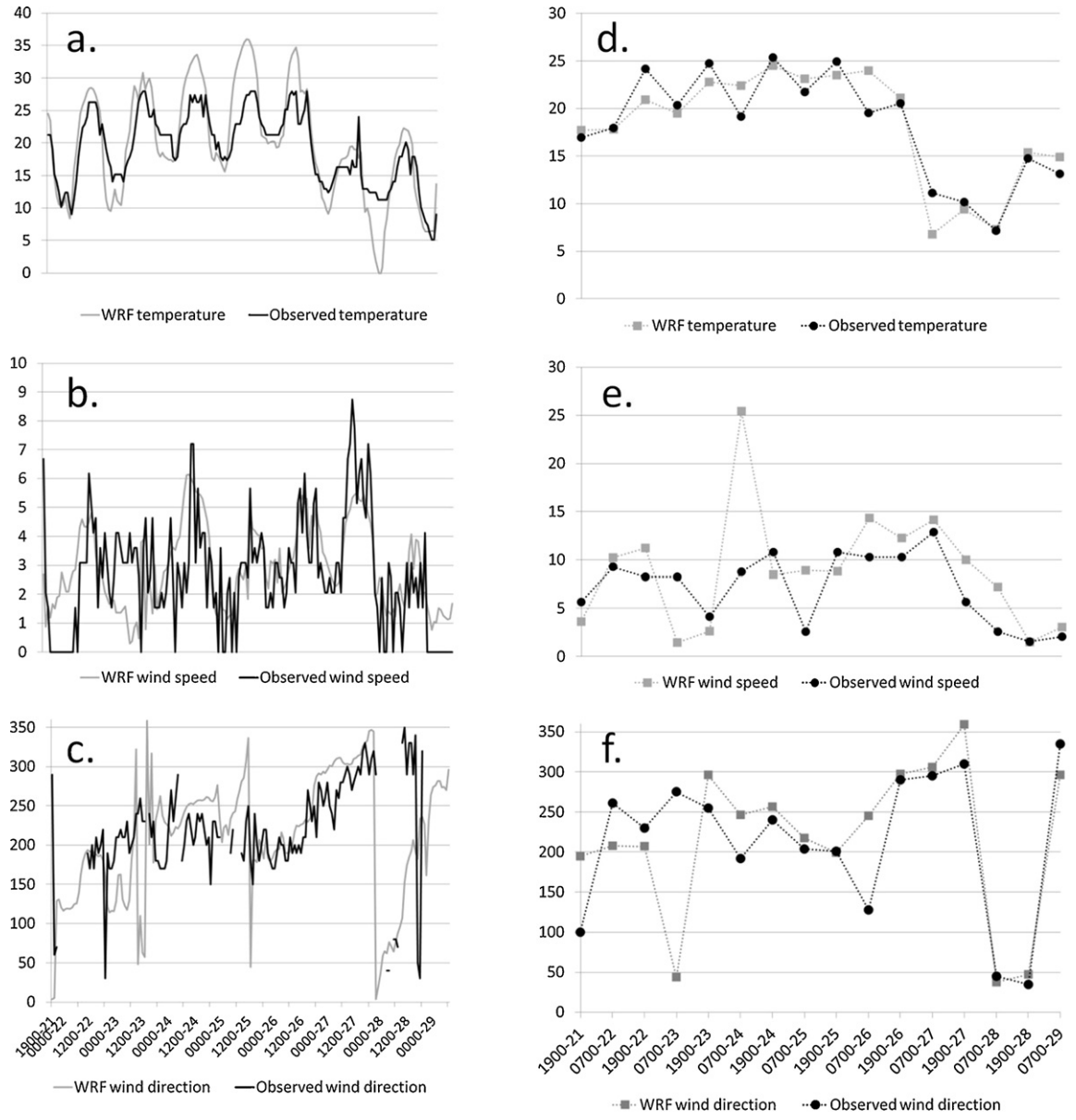

Fig. 10. Time series of simulated WRF (gray) weather conditions versus observed (black) weather conditions at the surface (a–c; Ely, MN, USA) and 800 m AGL (d–f; International Falls, MN, USA), respectively, from 1900 LDT 20 June through 1900 LDT 29 June 2007: (a) surface temperature (K), (b) surface wind speed ($m\,s^{-1}$), and (c) surface wind direction (degrees), (d) 800 m temperature (K), (e) 800 m wind speed ($m\,s^{-1}$), and (f) 800 m wind direction (degrees).

terminated prematurely due to the technical issue were excluded from analyses.

4. Discussion

4.1. Proof of concept evaluation

Dispersal distances simulated within this study indicate that the lakeshore sites are clearly within the dispersal range of SBW transport via the atmospheric pathway. This conclusion is not surprising given that SBW have been previously observed dispersing as far as 450 km (Greenbank et al., 1980). That particular observation occurred during an intense and widespread outbreak on northeastern mainland Canada, resulting in mass exodus over the Gulf of St. Lawrence and deposition of exhausted moths on the western shoreline of insular Newfoundland. By contrast, the deposition patterns simulated here should be representative of more common atmospheric transport that occurs during moderate and more localized outbreaks.

For strong fliers such as the SBW, the flight speed and the orientation of the insect relative to the transport wind can be significant factors affecting their final destination (Chapman et al., 2010). In the absence of wind, SBW is technically capable of straight-line flight distances of 7.2 km, 21.6 km, and 43.2 km given a rate of $2\,m\,s^{-1}$ in 1 h, 3 h, and 6 h, respectively. Hence a moth flying to exhaustion without wind assistance could fly approximately 50 km – not nearly enough to reach the lakeshore of Lake Superior from the defoliated source to the west in our case study. Yet SBW do not fly during calm winds, and when in exodus their flight direction is consistently in the downwind direction (Greenbank et al., 1980). The transport model integrates these factors along with other constraints (timing, precipitation, temperature, etc.) to replicate the dispersal behaviors Greenbank et al. observed over 30 years ago, supporting their conclusion that wind-mediated transport of SBW is fundamental to its dispersal capability, and the details of the meteorology during its

flight window have large implications for anisotropic long-distance dispersal in SBW.

Though the lakeshore sites were within the range of SBW atmospheric transport, the meteorological details underlying deposition patterns had large influence over the magnitude and direction of dispersal. The model indicated that emigration from the source to the lakeshore sites was plausible on just three of eight simulation dates. The limited extent of this localized outbreak resulted in relatively narrow moth deposition footprints on the lakeshore for the three immigration dates, so that immigration occurred on different dates across sites. Forced descent due to precipitation may have restricted dispersal of some moths to the northernmost lakeshore sites on 24 June, discussed in detail in the following section. Cool temperatures limited the dispersal distances to the east on 28 June when the deposition footprint extended to three of the lakeshore sites. These results emphasize how conditions at the time of dispersal can strongly affect the direction and distance travelled by actively dispersing SBW adults.

Our evaluation of the SBW atmospheric transport model is based on strong circumstantial evidence. BioSIM estimates of SBW phenology indicated that specimens captured within sites near the north shore of Lake Superior during the last week in June were unlikely to have been produced locally (Fig. 3). These model predictions are consistent with our larval collections over two different seasons (2006 and 2007, Sturtevant, unpublished data) and our adult trapping efforts (Fig. 6). Nonetheless we do not know the source of immigrants with certainty. The steepness of the environmental gradient near the lakeshore suggests that locations on the order of 10–20 km from the lakeshore could have conceivably contributed immigrants. These locations, however, had very low larval abundance and consequently had a low probability of contributing a sufficient number of dispersers to the target locations to match the observed patterns (see Anderson and Sturtevant, 2011). The closest inland location with defoliation and associated high larval abundance where phenology was sufficiently advanced in late June to produce emigrants was 150 km to the west. Trap captures along the lakeshore at the end of the flight window indicated presence rather than high densities (i.e., 10–20 adults per location). Likewise, simulations did not indicate any concentrated deposition of moths in the vicinity of the sites where trap captures would be expected to be substantially higher. As such, the simulation results strongly match both our local data and our understanding of SBW dispersal biology based on a detailed review of the literature.

4.2. Aerobiology insights

Simulations indicated that minimum temperature requirements and the premature descent caused by precipitation were the most important constraints on long-distance movements of SBW during the simulated dispersal window. Low temperatures can have a complex effect on dispersal behavior depending on the temperature profile above the ground surface (Achtemeier, 2002). SBW may encounter either cooler temperatures or warmer temperatures at higher altitudes depending whether an inversion layer develops (Dickison et al., 1986). In our specific case low temperatures affected lift-off most frequently later on cool nights as temperatures declined following sunset, with the lift-off failures starting around 2200 h on 21 and 22 June, and around 2000 h on 27 and 28 June. Earlier lift-off in response to cooler temperatures (Greenbank et al., 1980) may well be adaptive to offset minimum temperature constraints on flight.

Forced descent of moths by precipitation during SBW exodus events, similar to behavior illustrated by on 25 June simulation, has been observed for decades (Greenbank, 1957; Henson, 1951). The threshold level of precipitation required to force dispersing budworm from the sky is not known. Empirical observations of SBW in flight are problematic during rain events because it is difficult to distinguish moths from rain droplets (Dickison et al., 1986). Anecdotal evidence suggests that SBW do fly within rain cells (Dickison et al., 1986), and radar data clearly shows vertical displacement of moths in response to convective storms (Dickison et al., 1983, 1986; Greenbank et al., 1980). Spatial patterns of SBW landings in our study suggest that simulated rain affected the final distribution the SBW adults, possibly contributing to the divergent pattern of landings on the night of 24 June (Fig. 9b). Further research is needed to understand physical and behavioral responses of SBW adults to rainfall.

Other authors have reported that convergent meteorological processes can concentrate SBW moths within both airspace and deposition at the ground surface (e.g., Dickison et al., 1990). We observed little evidence of convergent meteorology activity during the dispersal window that we simulated. The exception was 26 June, when a concentrated band of SBW adults was deposited within Lake Superior (Fig. 7f). Deposition of these SBW adults was not due to either temperature or precipitation rules, therefore the cause of deposition was likely a low-level divergence area caused by the cold surface temperatures above the lake surface that drew SBW adults down from aloft. Hence while we have few examples of convergent activity from our limited dispersal window, the model did capture convergent wind fields and their consequences for deposition patterns of SBW.

The empirical altitudinal distribution (Schaefer, 1976) used to parameterize the initial level-off height of SBW adults was intended to represent typical cruising altitudes for dispersing moths under stable meteorological conditions (Dickison et al., 1986). Six of eight dates within the dispersal window showed maximum altitude distributions similar to Schaefer (1976), with varying degrees of expansion within the tail (Fig. 8b). On 24 and 25 June, when conditions were presumably unstable, the precipitation rule may have restricted the number of high altitude SBW adults. Maximum altitudes for SBW adults flying on 21 and 27 June suggested strong vertical uplift (Fig. 8b), but the range of altitudes observed (0–1000 m) remained consistent with the published studies of altitudinal profiles for SBW. Schaefer (1976) documented an increase in the mode altitude for vertical distributions of dispersing budworm through the nighttime hours as lower air masses became cooler. Our model assumes no behavioral response of SBW to air temperature other than minimum and maximum temperature constraints. This assumption may serve as a null model for the evaluation of SBW behaviors, such as mid-flight ascent triggered by cooler temperatures, to determine if temporal changes in altitude are either exclusively physical or modified by behavior. For example, flight patterns within the model were consistent with the physical turning and acceleration of wind with altitude in the planetary boundary layer (i.e., the Ekman spiral, Isard and Gage, 2001) (Figs. 8 and 9) that were also documented by Schaefer (1976). Since flying altitude can influence dispersal distance and direction, understanding the physical and behavioral processes affecting flight altitude are important.

Our application indicated that some modeled constraints had little influence on deposition patterns during the limited window for which we simulated dispersal. Very few SBW adults failed to lift-off due to temperatures in excess of 29.5 °C, and no SBW adults failed to lift-off due to calm winds during the our simulated flight period. Analysis of egg recruitment data by Régnière and Nealis (2007) suggests that moths are more likely to emigrate when evening wind conditions are unstable, consistent with our rule of a minimum wind speed constraint on lift-off. In our case, WRF appears to underestimate the frequency of calm nights (Fig. 10b). Hence this constraint may well have affected lift-off on 27 and 28 June, when surface records indicated calm nights.

4.3. Implications for population dynamics

Dispersal remains one of the most enigmatic processes affecting the population dynamics of insect pests (Régnière and Nealis, 2007). Atmospheric transport models such as the one presented here quantifies expected spatial patterns of insect movements under a given set of atmospheric conditions. Empirical observations – particularly those that can separate immigrants from locally-produced insects – are needed to validate such models. While immigration is known to influence local outbreak dynamics of SBW (Nealis and Régnière, 2004), methods are needed to quantify the relative contribution of emigration and immigration for year to year variation in population density at scales relevant to insect outbreaks. Research in agricultural systems–most notably migratory locust swarms in Africa and Asia (Latchininsky and Sivanpillai, 2010; Skaf et al., 1990) – provide examples where understanding atmospheric processes have significantly enhanced integrated pest management at international scales. Knowledge of both the dispersal process and its consequence on the spatiotemporal dynamics of forest insect populations may therefore have important ramifications for forest management and outbreak suppression strategies.

Anderson and Sturtevant (2011) applied hierarchical Bayesian modeling methods to 2007 SBW larvae and moth data in our study area to understand factors underlying adult male SBW movements over the entire dispersal season. They found that adult dispersal patterns were strongly directional at the scale of the full dispersal season, with flow from the northwest to the southeast. Our simulations suggest a broader range of dispersal directions, ranging from north to south, but not to the west. We attribute the discrepancy in direction to the differences in temporal resolution, and the fact that the current study focused on early dispersal where only a subset of the population was available for migration. Regardless of their differences, each study indicates directional bias in the long-distance movements of adult SBW that may have important spatial ramifications for population dynamics in this area.

Understanding spatial processes affecting atmospheric transport of SBW is dependent in part on identifying source populations and knowing the spatial distribution of susceptible host trees (i.e., destination habitats). Until recently these elements could only be coarsely estimated. Recent advances in remote sensing now allow mapping of both host tree species and insect defoliation with greater accuracy and at much finer spatial and temporal scales than previously available (de Beurs and Townsend, 2008; Townsend et al., 2012; Wolter and Townsend, 2011). In this study we used mapped distributions of spruce and fir to define potential destination habitats (Wolter et al., 2008). Such tree species-level mapping was critical since the forests in this region contain mixed conifer-deciduous tree composition, and less detailed land-cover classifications could not have separated non-host conifers (i.e., pines and cedar) from host tree species (fir and spruce).

Search mechanisms by which SBW locate and immigrate to locations with either females for mating or suitable host trees for oviposition are poorly understood. Observations documented by Greenbank et al. (1980) suggest that SBW fold their wings and drop from the sky when passing over suitable habitat. We approximated that process within the model as SBW adults searching for host drop from the sky at their terminal velocity when directly above host targets. We anticipated that the abundance of available host in the direction of dispersal would have strong influence over the ability of SBW to successfully land within host. If true, then we expect greater dispersal losses over areas where host are less abundant and poorly connected, with potential population-level consequences. Our simulations indicate that atmospheric processes at play during the time of dispersal may override the effect of host patterns on dispersal success. Over our short eight-day dispersal window, factors such as wind speed, cool temperatures, and precipitation affected landing success, even when SBW adults were flying over areas with abundant host (Table 3).

4.4. Model limitations

The SBW atmospheric transport model demonstrated complex and realistic dispersal behavior despite the simplicity of the rules governing SBW adult behavior relative to the range of evolutionary and meteorological factors that potentially could be involved. While the simulations were consistent with our ground data, a full evaluation of model behavior would require significant data resources such as radar-derived insect density profiles or marked specimens where the source and destinations of long-distance migrants are known with certainty. In lieu of such data resources, we identify a few important shortcomings of the approach that may decrease our certainty in the model projections.

Vertical velocity is simulated explicitly in the WRF using a prognostic equation for the vertical component of momentum, and can occur as a result of many physical processes including air flow over uneven terrain, inertial waves, surface convergence, and convective updrafts (Skamarock et al., 2005). Terrain in the study area is relatively flat, dominated by fine-scaled heterogeneity that is generally of limited influence at the 4 km resolution of the WRF model outputs. An exception is the steep topography along the lakeshore of Lake Superior (Fig. 9b) that was approximated within the WRF environment. Studies of avian flight demonstrate the importance of orographic wind deflection on flight patterns (Brandes and Ombalski, 2004). It is therefore possible that the resolution of the weather outputs affected our results.

We did not include sub-gridscale turbulence within the SBW atmospheric transport model, in part because convective turbulence is minimized by the stability of the nocturnal conditions when SBW adults fly, since the ground surface is no longer heated by solar radiation (Storm et al., 2009). The remaining turbulence is mechanical, caused by friction with the ground surface (trees, etc.). Such processes have been shown to influence the wind dispersal of seeds (Bohrer et al., 2008) at scales from 10^1 to 10^3 m. Simulated dispersal distances of SBW adults were 1–3 orders of magnitude larger than this range, suggesting such fine-scaled mechanical turbulence acts primarily as white noise at this scale that integrates out over time. Indeed the empirical flight parameters estimated by Greenbank et al. (1980) were intended to capture the effects of synoptic weather patterns (e.g., Dickison et al., 1983, 1986, 1990), rather than fine-scaled turbulence, on dispersal patterns of SBW. Guichard et al. (2012) used an agent-based modeling approach analogous to ours to examine moth dispersal patterns at higher resolution than that simulated here, but required empirical data collected as similarly fine spatial scales.

Precipitation within the WRF model reflects simulated rainfall rather than actual observed precipitation. Hence we cannot say for certain that precipitation simulated by the WRF model actually occurred precisely at a given time, place, and height, because of an inexact match between meteorological measurements and model results, and model temporal and spatial resolution. Since actual rainfall tends to be more heterogeneous in time and space (Skamarock et al., 2005), the most precise conclusion we can make is that the model suggests atmospheric conditions conducive to rain production occurred in some locations in the study area at that time. For example, the temporal resolution of rainfall in the model is one hour, but could have occurred lightly for one hour or heavily in a few minutes. Spatial interpolation within the model also spreads a given amount of precipitation over a greater area within the simulations than may have occurred. This limitation is important because storm activity is known to be an important factor affecting dispersal distance, and the process of “washing out” insects from the sky is likely to be nonlinear (Dickison et al., 1983,

1986). Finally, the amount of precipitation necessary to force flying SBW from the sky is not known – only that budworm have both been observed in flight during heavy rains and observed washing out at ground level (Dickison et al., 1986; Greenbank et al., 1980).

Our estimates of landing success are at best an approximation how SBW actually detect and land within areas of suitable host trees. While Greenbank et al. (1980) suggest that budworm sense host below them, the search mechanisms by which budworm detect host while aloft are not known, nor is it known whether males use either host or pheromone cues to detect mates while dispersing. We also do not know the extent to which SBW actively fly toward targets following descent. Evidence suggests that SBW adults forced to land within nonforested habitat will make subsequent short-distance flights in search of nearby host (Greenbank et al., 1980). Finally, we defined host targets as locations where the combination of spruce and fir were dominant (i.e., greater than 50% of the basal area). However balsam fir is sparsely distributed over the majority of the study area (Wolter et al., 2008), to the extent that "successful" dispersal was difficult to define.

Our design and parameterization of the SBW atmospheric transport model are based exclusively on the long-term and extensive datasets collected for SBW in New Brunswick Canada. The physical processes affecting the atmospheric transport of budworm are transferable across systems. However the extent to which behavioral and physiological responses of SBW vary across its range is not known. Sensitivity analyses may also provide insights into how our parameter choices affected model behavior. However a true sensitivity analysis requires a broader range of meteorological conditions than our eight-day dispersal window allowed, and is therefore beyond the scope of the model demonstration provided here.

5. Conclusions

Our SBW atmospheric transport model provides opportunity to examine exodus flight behaviors of SBW at spatial and temporal resolutions that were previously only possible via coordinated ground and radar-based studies. Insights from model results may be compared with past empirical observations of flight behavior of SBW within the atmosphere, and suggest future efforts necessary to address key uncertainties in SBW flight behavior. These uncertainties include behavioral responses of SBW to vertical heterogeneity in air temperature, search mechanisms and resulting success rates for locating suitable host for either mating (males) or oviposition (females), the amount of precipitation necessary to force descent of flying SBW from the air column, and other mechanisms of vertical displacement.

Aerobiology has been suggested as a critical frontier in integrated pest management and national biosecurity (Gage et al., 1999). The fact that we were able to apply SBW flight responses to meteorological conditions documented over thirty years ago to simulate a modern migration event is a testament to the value of basic aerobiological research. SBW is among the few insect species for which active flight behaviors have been studied in situ in sufficient detail to parameterize an atmospheric transport model. However rapid advances in insect tracking technologies continue to improve our ability to study such processes under field conditions (Isard and Gage, 2001). In parallel, behavioral entomologists have developed techniques and specialized equipment (e.g., flight mills) to empirically estimate key flight behaviors, parameters, and constraints for a variety of flying insects in laboratory settings (Lu et al., 2007; Vogt et al., 2000; Wu et al., 2006). After accounting for bias introduced by artificial lab settings (Riley et al., 1997), such studies provide information needed to parameterize analogous agent-based flight models of the atmospheric transport of insects. Methods that allow definitive separation of immigrants from locally-produced individuals will further improve the capacity to validate atmospheric transport models by clearly defining insect immigration events in time and space, while advances in remote sensing technology can more accurately map the terrestrial environment over which they disperse. Such research may ultimately inform the decades-long debate of how long-distance dispersal contributes to spatiotemporal dynamics of insect outbreaks, particularly as irruptive populations interact with earth systems increasingly modified for human use.

Acknowledgments

This work was supported by the United States Department of Agriculture, Cooperative State Research Education and Extension Service, National Research Initiative Grant no. WISR-2005-02815, and funding from the US National Fire Plan. Atmospheric modelling was initiated under the National Fire Plan 01.SRS.A.5. We would to thank the following people for assisting with the field data collection: Nate Aspelin, Louis-Etienne Robert, Brian Miranda, Robert Costanza, Stephane Bourassa, and Patrick James. The Superior National Forest provided housing during the field season and assisted with sampling logistics. We also thank Scott Isard, Andrew Liebhold and two anonymous reviewers for their valuable comments on earlier versions of the manuscript. Finally we wish to dedicate this paper to the memory of David Greenbank, whose pioneering work on long-distance insect dispersal made this study possible.

References

Achtemeier, G.L., 1979. Evaluation of operational streamline methods. Monthly Weather Rev. 107, 198–206.
Achtemeier, G.L., 1996. The maiden flight of ten thousand mechanical bugs, 12th Conference on Biometeorology and Aerobiology. American Meteorological Society, Atlanta, GA, pp. 425–429.
Achtemeier, G.L., 2002. Interface modeling for atmospheric transport of biota, 15th Conference on Biometeorology and Aerobiology and 16th International Conference of Biometeorology. American Meteorological Society and International Society of Biometeorology, Kansas City, MO, USA, pp. 204–208.
Anderson, D.P., Sturtevant, B.R., 2011. Pattern analysis of eastern spruce budworm *Choristoneura fumiferana* dispersal. Ecography 34, 488–497.
Bohrer, G., Katul, G.G., Nathan, R., Walko, R.L., Avissar, R., 2008. Effects of canopy heterogeneity, seed abscission and inertia on wind-driven dispersal kernels of tree seeds. J. Ecol. 96, 569–580.
Bohrerova, Z., Bohrer, G., Cho, K.D., Bolch, M.A., Linden, K.G., 2009. Determining the viability response of pine pollen to atmospheric conditions during long-distance dispersal. Ecol. Appl. 19, 656–667.
Brandes, D., Ombalski, D.W., 2004. Modeling raptor migration pathways using a fluid-flow analogy. J. Raptor Res. 38, 195–207.
Canadian Council on Geomatics, 2009. GeoBase. http://www.geobase.ca/geobase/en/index.html (February 2009).
Chapman, J.W., Nesbit, R.L., Burgin, L.E., Reynolds, D.R., Smith, A.D., Middleton, D.R., Hill, J.K., 2010. Flight orientation behaviors promote optimal migration trajectories in high-flying insects. Science 327, 682–685.
Chen, F., Dudhia, J., 2001. Coupling an advanced land-surface/hydrology model with the Penn State/NCAR MM5 modeling system. Part I: Model implementation and sensitivity. Monthly Weather Rev. 129, 587–604.
Cooke, B.J., Roland, J., 2000. Spatial analysis of large-scale patterns of forest tent caterpillar outbreaks. Ecoscience 7, 410–422.
de Beurs, K.M., Townsend, P.A., 2008. Estimating the effect of gypsy moth defoliation using MODIS. Remote. Sens. Environ. 112, 3983–3990.
Dickison, R.B.B., Haggis, M.J., Rainey, R.C., 1983. Spruce budworm moth flight and storms: case study of a cold front system. J. Appl. Meteorol. 22, 278–286.
Dickison, R.B.B., Haggis, M.J., Rainey, R.C., Burns, L.M.D., 1986. Spruce budworm moth flight and storms, further studies using aircraft and radar. J. Appl. Meteorol. 25, 1600–1608.
Dickison, R.B.B., Mason, P.J., Browning, K.A., Lunnon, R.W., Pedgley, D.E., Riley, J.R., Joyce, R.J.V., 1990. Detection of mesoscale synoptic features associated with dispersal of spruce budworm moths in eastern Canada. Philos. Trans. R. Soc. Lond. Ser. B 328, 607–617.
Dudhia, J., 1989. Numerical study of convection observed during the winter monsoon experiment using a mesoscale two-dimensional model. J. Atmos. Sci. 46, 3077–3107.
Environment Canada, 2009. National Climate Data and Information Archive. www.climate.weatheroffice.gc.ca

Fossberg, M.A., Peterson, M., 1986. Modeling airborne transport of gypsy moth (Lepidoptera: Lymantridae) larvae. Agric. For. Meteorol. 38, 1–8.
Gage, H.S., Isard, A.S., G-Colunga, M., 1999. Ecological scaling of aerobiological dispersal processes. Agric. For. Meteorol. 97, 249–261.
Greenbank, D.O., 1957. The role of climate and dispersal in the initiation of outbreaks of the spruce budworm in New Brunswick. II. The role of dispersal. Can. J. Zool. 35, 385–403.
Greenbank, D.O., Schaefer, G.W., Rainey, R.C., 1980. Spruce budworm (Lepidoptera: Tortricidae) moth flight and dispersal: new understanding from canopy observations, radar, and aircraft. Mem. Entomol. Soc. Can. 110, 1–49.
Guichard, S., Kriticos, D.J., Leriche, A., Kean, J.M., Worner, S.P., 2012. Individual-based modelling of moth dispersal to improve biosecurity incursion response. J. Appl. Ecol. 49, 287–296.
Heinselman, M.L., 1973. Fire in the virgin forests of the Boundary Waters Canoe Area, Minnesota. J. Quater. Res. 3, 329–382.
Henson, W.R., 1951. Mass flights of the spruce budworm. Can. Entomol. 83, 240.
Isard, S.A., Gage, H.S., Comtois, P., Russo, J.M., 2005. Principles of the atmospheric pathway for invasive species applied to soybean rust. BioScience 55, 851–862.
Isard, S.A., Gage, S.H., 2001. Flow of Life in the Atmosphere: An Airscape Approach to Understanding Invasive Organisms. Michigan State University Press, East Lansing, MI.
Isard, S.A., Russo, J.M., Ariatti, A., 2007. The integrated aerobiology modeling system applied to the spread of soybean rust into the Ohio River valley during September 2006. Aerobiologia 23, 271–282.
Janjic, Z.I., 1996. The Surface Layer in the NCEP Eta Model, in 11th Conference on NWP, edited, pp. 354–355, American Meteorological Society, Norfolk, VA.
Janjic, Z. I. 2002. Nonsingular Implementation of the Mellor-Yamada Level 2.5 Scheme in the NCEP Meso model, edited, NCEP Office Note No. 437, p. 61.
Kain, J.S., Fritsch, J.M., 1993. Convective parameterization for mesoscale models: The Kain–Fritsch scheme. The Representation of Cumulus Convection in Numerical Models, in Meteor. Monogr., edited, pp. 165–170, Amer. Meteor. Soc.
Keyghobadi, N., LaPointe, D., Fleischer, R.C., Fonseca, D.M., 2006. Fine-scale population genetic structure of a wildlife disease vector: the southern house mosquito on the island of Hawaii. Mol. Ecol. 15, 3919–3930.
Keyghobadi, N., Roland, J., Strobeck, C., 1999. Influence of landscape on the population genetic structure of the alpine butterfly *Parnassius smintheus* (Papilionidae). Mol. Ecol. 8, 1481–1495.
Latchininsky, A.V., Sivanpillai, R., 2010. Locust habitat monitoring and risk assessment using remote sensing and GIS technologies. In: Ciancio, A., Mukerji, K.G. (Eds.), Integrated Management of Arthropod Pests and Insect Borne Diseases. Integrated Management of Plant Pests and Diseases. Springer, Netherlands, pp. 163–188.
Lin, Y.-L., Farley, R.D., Orville, H.D., 1983. Bulk parameterization of the snow field in a cloud model. J. Clim. Appl. Meteorol. 22, 1065–1092.
Lu, Y., Wu, K., Guo, Y., 2007. Flight potential of *Lygus lucorum* (Meyer-Dvr) (Heteroptera: Miridae). Environ. Entomol. 36, 1007–1013.
Mandel, J.T., Bildstein, K.L., Bohrer, G., Winkler, D.W., 2008. Movement ecology of migration in turkey vultures. Proc. Natl. Acad. Sci. U. S. A. 105, 19102–19107.
Mandel, J.T., Bohrer, G., Winkler, D.W., Barber, D.R., Houston, C.S., Bildstein, K.L., 2011. Migration path annotation: cross-continental study of migration-flight response to environmental conditions. Ecol. Appl. 21, 2258–2268.
Mellor, G.L., Yamada, T., 1982. Development of a turbulence closure model for geophysical fluid problems. Rev. Geophys. Space Phys. 20, 851–875.
Mesinger, F., DiMego, G., Kalnay, E., Mitchell, K., Shafran, P.C., Ebisuzaki, W., Jović, D., Woollen, J., Rodgers, E., Berbery, E.H., Ek, M.B., Fan, Y., Grumbine, R., Higgins, W., Li, H., Lin, Y., Manikin, G., Parrish, D., Sh, W., 2006. North American Regional Reanalysis. Bull. Am. Meteorol. Soc. 87, 343–360.
Mlawer, E.J., Taubman, S.J., Brown, P.D., Iacono, M.J., Clough, S.A., 1997. Radiative transfer for inhomogeneous atmosphere: RRTM, a validated correlated-k model for the longwave. J. Geophys. Res. Atmos. 102, 16663–16682.
Mullen, M.A., Wileyto, E.P., Arthur, F.H., 1998. Influence of trap design and location on the capture of *Plodia interpunctella* (Indian meal moth) (Lepidoptera: Pyralidae) in a release-recapture study. J. Stored Prod. Res. 34, 33–36.
Nathan, R., Sapir, N., Trakhtenbrot, A., Katul, G.G., Bohrer, G., Otte, M., Avissar, R., Soons, M.B., Horn, H.S., Wikelski, M., Levin, S.A., 2005. Long-distance biological transport processes through the air: can nature's complexity be unfolded in silico? Divers. Distrib. 11, 131–137.
National Oceanic and Atmospheric Administration, 2009. National Climatic Data Center. http://www.ncdc.noaa.gov/oa/ncdc.html (February 2009).
Nealis, V.G., Régnière, J., 2004. Fecundity and recruitment of eggs during outbreaks of the spruce budworm. Can. Entomol. 136, 591–604.
Onstad, W.D., Crwoder, W.D., Isard, A.S., Levine, E., Spencer, L.J., O'Neal, E.M., Ratcliffe, T.S., Gray, E.M., Bledsoe, W.L., Fonzo Di, D.C., Eisley, B.J., Edwards, R.C., 2003. Does landscape diversity slow the spread of rotation-resistant western corn rootworm (Coleoptera: Chrysomelidae)? Environ. Entomol. 32, 992–1001.
Régnière, J., Amant-Saint, R., 2004. User's Manual BioSim 8.0. Natural Resources Canada Canadian Forest Service-Quebec, pp. 1–84.
Régnière, J., Nealis, V.G., 2007. Ecological mechanisms of population change during outbreaks of the spruce budworm. Ecol. Entomol. 32, 461–477.
Régnière, J., You, M., 1991. A simulation model of spruce budworm (Lepidoptera, Tortricidae) feeding on balsam fir and white spruce. Ecol. Model. 54, 277–297.
Riley, J.R., Downham, M.C.A., Cooter, R.J., 1997. Comparison of the performance of *Cicadulina leafhoppers* on flight mills with that to be expected in free flight. Entomol. Exp. Appl. 83, 317–322.
Riley, J.R., Xia-Nian, C., Xiao-Xi, Z., Reynolds, D.R., Guo-Min, X., Smith, A.D., i-Yi, C., Ai-Dong, B., Bao-Ping, Z., 1991. The long distance migration of *Nilaparvata lugens* (Stål) (Delphacidae) in China: radar observations of mass return flight in the autumn. Ecol. Entomol. 16, 471–489.
Royama, T., 1979. Effect of adult dispersal on the dynamics of local populations of an insect species: a theoretical investigation. In: Berryman, A.A., Safranyk, L. (Eds.), Proceedings of the Second IUFRO Conference: Dispersal of Forest Insects: Evaluation, Theory and Management Implications. Washington State University, Pullman, Washington, USA, pp. 79–93.
Royama, T., 1984. Population dynamics of the spruce budworm *Choristoneura fumiferana*. Ecol. Monogr. 54, 429–462.
Royama, T., MacKinnon, W.E., Kettela, E.G., Carter, N.E., Hartling, L.K., 2005. Analysis of spruce budworm outbreak cycles in New Brunswick, Canada, since 1952. Ecology 86, 1212–1224.
Sanders, C.J., Wallace, D.R., Lucuik, G.S., 1978. Flight activity of female eastern spruce budworm (Lepidoptera, Tortricidae) at constant temperatures in the laboratory. Can. Entomol. 107, 1289–1299.
Sapir, N., Horvitz, N., Wikelski, M., Avissar, R., Mahrer, Y., Nathan, R., 2011. Migration by soaring or flapping: numerical atmospheric simulations reveal that turbulence kinetic energy dictates bee-eater flight mode. Proc. R. Soc. B-Biol. Sci. 278, 3380–3386.
Schaefer, G.W., 1976. Radar observations of insect flight. In: Rainey, R.C. (Ed.), Insect Flight. John Wiley and Sons, New York, pp. 157–197.
Schueler, S., Schlunzen, K.H., 2006. Modeling of oak pollen dispersal on the landscape level with a mesoscale atmospheric model. Environ. Model. Assess. 11, 179–194.
Scott, R.W., Achtemeier, G.L., 1987. Estimating pathways of migrating insects carried in atmospheric winds. Environ. Entomol. 16, 1244–1254.
Shamoun-Baranes, J., Leyrer, J., van Loon, E., Bocher, P., Robin, F., Meunier, F., Piersma, T., 2010. Stochastic atmospheric assistance and the use of emergency staging sites by migrants. Proc. R. Soc. B-Biol. Sci. 277, 1505–1511.
Skaf, R., Popov, G.B., Roffey, J., Scorer, R.S., Hewitt, J., 1990. The desert locust: an international challenge [and discussion]. Philos. Trans. R. Soc. Lond. Ser. B 328, 525–538.
Skamarock, W.C., Klemp, J.B., Dudhia, J., Gill, D.O., Barker, D.M., Wang, W., Powers, J.G., 2005. A description of the advanced research WRF Version 2. NCAR technical note.
Storm, B., Dudhia, J., Basu, S., Swift, A., Giammanco, I., 2009. Evaluation of the weather research and forecasting model on forecasting low-level jets: implications for wind energy. Wind Energy 12, 81–90.
Strand, J.F., 2000. Some agrometeorological aspects of pest and disease management for the 21st century. Agric. For. Meteorol. 103, 73–82.
U.S. Forest Service, 2007. Forest Health Monitoring aerial detection annual surveys. http://www.fs.fed.us/foresthealth/technology/ads_standards.shtml (January 2008).
U.S. Geologic Survey, 2009. National Elevation Dataset (NED). http://eros.usgs.gov/#/Find_Data/Products_and_Data_Available/NED (February 2009).
Vogt, J.T., Appel, A.G., West, M.S., 2000. Flight energetics and dispersal capability of the fire ant, *Solenopsis invicta* Buren. J. Insect Physiol. 46, 697–707.
Waggoner, E.P., Aylor, E.D., 2000. Epidemiology: a science of patterns. Ann. Rev. Phytopathol. 38, 71–94.
Westbrook, K.J., Isard, A.S., 1999. Atmospheric scales of biotic dispersal. Agric. For. Meteorol. 97, 263–274.
Williams, D.W., Liebhold, A.M., 2000. Spatial synchrony of spruce budworm outbreaks in eastern North America. Ecology 81, 2753–2766.
Townsend, P.A., Singh, A., Foster, J.R., Rehberg, N.J., Kingdon, C.C., Eshleman, K.N., Seagle, S.W., 2012. A general Landsat model to predict canopy defoliation in broadleaf deciduous forests. Remote. Sens. Environ. 119, 255–265.
Wolter, P.T., Townsend, P.A., 2011. Multi-sensor data fusion for estimating forest species composition and abundance in northern Minnesota. Remote. Sens. Environ 115, 671–691.
Wolter, P.T., Townsend, P.A., Sturtevant, B.R., Kingdon, C.C., 2008. Remote sensing of the distribution and abundance of host species for spruce budworm in Northern Minnesota and Ontario. Remote. Sens. Environ. 112, 3971–3982.
Wu, H., Wu, K., Wang, D., Guo, Y., 2006. Flight potential of pink bollworm, *Pectinophora gossypiella* Saunders (Lepidoptera: Gelechiidae). Environ. Entomol. 35, 887–893.